International Journal of Applied Science and Engineering

Extraction optimization of antifungal from *Momordica charantia* seeds against green mold disease in mushroom cultivation

Muhamad Ikmal Sirozi [1*], Noor Hasyierah Mohd Salleh [1,2*], Zarina Zakaria [1,2], Norhidayah Abd Aziz [1], Siti Aminah Hassan [1,2], Mohd Amin Zainal Abidin [3]

[1] *Faculty of Chemical Engineering & Technology, Universiti Malaysia Perlis, 02600, Arau, Perlis, Malaysia*
[2] *The Centre of Excellence for Biomass Utilization, Universiti Malaysia Perlis, 02600, Arau, Perlis, Malaysia*
[3] *Beseri Agrofarm Resources, No. 10, Lorong BD 4, Kampung Beseri Dalam, 02400, Beseri, Perlis, Malaysia*

ABSTRACT

Gray oyster mushroom cultivation continuously suffers from green mold diseases mainly caused by *Trichoderma* spp. in which the infection has caused a reduction in cropping quantity, production, and harvest quality, which has led to substantial mushroom yield decreases and economic repercussions. *Trichoderma* spp. has been identified for its pathogenic potential on mushrooms and also other agricultural products, which highlights the necessity for an effective control strategy to mitigate green mold disease infection. *Momordica charantia* seeds are waste produced from food processing consisting of a high protein concentration and have been reported as a potent antifungal agent against *Fusarium oxysporum.* However, the protein of *M. charantia* seed extract has not been optimized despite its effectiveness as well as its antifungal activity against *Trichoderma* spp. is not well discovered. Hence, the primary objective of this research is to optimize the *M. charantia* seed protein extract (MSPE) using ultrasound-assisted extraction (UEA) and to assess its antifungal properties against *Trichoderma* spp. In this study, the optimal protein concentration was 22.80 mg/mL, which was attained by using 1.58 M NaCl, 0.3 solute-to-solvent (g/mL), and 7.68 minutes extraction time. The TPC and TFC of the MSPE were 16.45 mg GAE/g extract and 5.78 mg NE/g extract, respectively. From the isolation of the infected mushroom bag, *Trichoderma* sp. ZH1 (Accession no.: DQ282127) was the closest species. The maximum inhibition of MSPE towards *Trichoderma* sp. ZH1 was 75.44% at 22.50 mg/mL. The LC_{50} and LC_{90} values were 13.62 mg/mL and 24.97 mg/mL respectively. The MGI and SGI at LC_{50} were 52.91% and 55% respectively. The current study indicated that MSPE significantly influenced the reduction of mycelium growth, and spore germination *in vitro*. Therefore, this study demonstrated the *M. charantia* seed extract's efficacy in controlling *Trichoderma* sp. ZH1 in mushroom cultivation and can be potentially applied as a green alternative for better mushroom disease management.

Keywords: *Trichoderma* spp., Gray oyster mushroom, *Momordica charantia* seed, Protein extraction, Optimization.

OPEN ACCESS

Received: December 6, 2023
Revised: January 22, 2024
Accepted: January 28, 2024

Corresponding Author:
Muhamad Ikmal Sirozi
m.ikmalsirozi@gmail.com
Hasyierah Mohd Salleh
hasyierah@unimap.edu.my

Publisher:
Chaoyang University of Technology
ISSN: 1727-2394 (Print)
ISSN: 1727-7841 (Online)

1. INTRODUCTION

Mushrooms are globally renowned as a top superfood choice due to their outstanding nutritional value. The market demand for mushrooms grows yearly because customers

prefer vegan or unprocessed foods rather than processed foods. Among all types of mushrooms, the gray oyster mushroom (*Pleurotus pulmonarius*) has a high demand from consumers worldwide. However, mushroom cultivation is constantly affected by several mushroom diseases, such as green mold disease from *Trichoderma* spp. (Bellettini et al., 2019). The super spreader of *Trichoderma* spp. easily takes over *P. pulmonarius* growth, consequently causing qualitative and quantitative losses in mushroom production (Santra and Banarjee, 2020). The most common control method used is chemical fungicides. However, this approach has contributed to several environmental and health concerns. Currently, many alternatives have been explored, including antagonistic microorganisms, plant extracts and essential oils, bio fungicides, chitosan and chitosan-based citrus coatings, heat treatments, ionizing and nonionizing irradiations, synthetic elicitors, and food additives as potential solutions to address this issue (Bhatta, 2021).

The effectiveness of antifungal plant extract is comparable to commercial chemical fungicides besides value for money, environmentally friendly, and minimal human health issues. *Momordica charantia*, also known as bitter melon or bitter gourd, is a well-established use as a medicinal plant. The bioactive compounds like phenolic compounds were found in the plant parts (seeds, stems, roots, leaves, and fruits) of *M.* charantia and their antifungal activities have been examined. According to previous studies, the *M.* charantia extract has shown significant inhibition against several types of pathogens (*Fusarium solani*, *Bipolaris maydis*, *Fusarium graminearum*, *Aspergillus oryzae*, *Aspergillus niger*, and *Sclerotinia sclerotiorum*) (Zhu et al., 2013; Wang et al., 2016).

Apart from that, the seeds of *M.* charantia, a by-product during its processing, contain an alpha-momorcharin (α-MMC) compound, which is a ribosome-inactivating protein (RIP) (Chen et al., 2019). RIPs have gained the attention of researchers because of their versatile effects on both plant and animal cells, as antifungal, antioxidant, antimicrobial, antihyperglycemic, and anticancer purposes (Chen et al., 2019; Villarreal-La et al., 2020).

Ultrasound-assisted extraction (UAE) has a higher potential output than conventional extraction. Sonication boosts the extraction of bioactive components from natural sources to a solvent medium through the synergistic effects of cavitation, mechanical agitation, and thermal processes (Azmir et al., 2019). The utilization of UAE is a straightforward, easy, and affordable method that allows the reduction in solvent consumption, process temperatures, and extraction times and improves extraction efficiency (Chemat et al., 2017).

Protein extractability is subject to several factors, including solvent concentration, extraction duration, solute-to-solvent ratio, pH, and temperature. The yield is influenced not only by individual factors but also by their collective impact. Response surface methodology (RSM) is a statistical approach that effectively utilizes processes in situations with consideration of multiple parameters and their interactions impact consideration on the desired experimental outcomes. Optimizing protein extraction can improve process management and product quality. Consequently, the current study aims to improve the protein extraction process of *M. charantia* seeds and assess the protein extract's antifungal properties against *Trichoderma* spp. through *in-vitro* analysis. The protein extract obtained from *M. charantia* seeds may present an alternative strategy for managing and controlling green mold disease infections in mushroom cultivation. It could potentially serve as an environmentally friendly substitute for synthetic fungicides for controlling fungal pathogens in agricultural crop fields.

2. MATERIALS AND METHODS

2.1 Plant Material Preparation and Reagents

Dried F1 hybrid mini bitter gourd seeds were utilized and obtained from Leckat Corporation Sdn Bhd, located in Kuala Lumpur, Malaysia. The reagents, chemicals, and solvents employed, including Bradford reagent, bovine serum albumin (BSA), n-hexane, sodium chloride, hydrochloric acid, sodium hydroxide, and sodium phosphate buffer, were all analytical standards and were obtained from Sigma-Aldrich, USA. The glassware was thoroughly cleaned with double-distilled water before and after use.

2.2 Ultrasound-Assisted Protein Extraction

The pink seeds were initially cut into smaller pieces using a 5.5-inch utility knife (specifically, the Chicago Cutlery brand). Afterward, it was processed into a powder form using a Panasonic MX-801S grinder and then passed through a sieve to achieve a fine and consistent particle size of 0.71 mm, following the method outlined by Tan et al. (2014). The fat content of the M. charantia seeds was removed by using n-hexane at a ratio of 1 : 3 (weight per volume). The mixture was continuously stirred for a duration of 3–4 h, maintaining a temperature range of 40 ± 2°C as described in the procedure by Horax et al. (2011). Afterward, the mixture underwent filtration and was dried in a fume hood to ensure that any residual n-hexane was completely removed. Finally, the seed powder was subsequently stored inside an airtight bag with silica gel for further analysis.

The powder of defatted *M.* charantia seeds was mixed with NaCl solution and subjected to ultrasonic extraction using a probe sonicator (Branson 450 Digital Sonifier Specifications) at a power of 90 W, frequency of 25 KHz, and a duty cycle of 75% (Gadalkar and Rathod, 2020). The sample was processed in a cold environment with a temperature of 10 ± 2°C and kept in a dark environment to

prevent exposure to light. Each experiment was replicated three times to ensure precise and reliable readings.

The protein concentration was measured via the Bradford assay method. Briefly, 1 mL of the MSPE was combined with 3 mL of Bradford reagent, and the mixture was thoroughly vortexed. It was then incubated at a temperature of 27°C for approximately 10 min. Subsequently, 1.5 mL of this mixture was transferred into a cuvette, and an absorbance reading was taken at 595 nm using a UV-visible spectrometer (Shimadzu UV-1800 ultraviolet-visible spectrophotometer). Each reading was performed three times to ensure accuracy. As a control, the MSPE volume was replaced with distilled water. All of these analyses were conducted in a dark environment. The protein obtained was further analyzed to determine the optimal experimental conditions for the MSPE. Bovine serum albumin was prepared and used to create a standard curve using the Bradford method.

2.3 Experimental design of response surface methodology (RSM)

The optimization of the *M. charantia* seed protein extract was conducted using RSM through a central composite design (CCD) setting with three center points. The correlation among the parameter variables NaCl concentration (0.32 to 2.67 M), solute-to-solvent ratio (0.05 to 0.55 g/mL), and extraction time (0.43 to 15.57 min) was studied based on the desired response, that is, protein concentration (mg/mL) (Table 1). The pH of the sodium chloride (NaCl) solution was modified to a pH of 9 by adding 0.1 M hydrochloric acid (HCl) or 0.1 M sodium hydroxide (NaOH).

The predicted response was analyzed using multiple regression analysis by following the second-order polynomial equation as presented in Equation (1), where Y_n denotes the response variables, β_o is the intercept, β_i is the linear regression coefficient, β_{ii} is the quadratic and β_{ij} is the cross-product term, x_i and x_j are the input variables, and k is the number of input variables (k = 3).

$$Y_n = \beta_o + \sum_{i=0}^{k} \beta_i x_i + \sum_{i=0}^{k} \beta_{ii} x_i^2 + \sum_{i=1}^{k} \sum_{j=i+1}^{k-1} \beta_{ij} x_i x_i. \quad (1)$$

The 17 runs consisted of 14 factorial points and 3 central points were randomly employed to investigate the MSPE concentration as tabulated in Table 2.

Table 1. Range of extraction condition for RSM

Independent variables	Parameter	Coded levels				
		-α	-1	0	1	+α
NaCl concentration	A	0.32	0.80	1.50	2.20	2.67
solute-to-solvent ratio	B	0.05	0.15	0.30	0.45	0.55
extraction time	C	0.43	3.50	8.00	12.50	15.57

Table 2. MSPE concentration obtained after optimization by central composite design (CCD)

Run	Factors			Response: MSPE concentration (mg/mL)
	A: NaCl concentration (M)	B: ratio (solute-to-solvent) (g/mL)	C: extraction time (min)	
1	2.20	0.15	3.50	7.21
2	2.20	0.45	12.50	3.66
3	2.20	0.15	12.50	3.59
4	1.50	0.30	15.57	1.65
5	0.80	0.45	12.50	5.34
6	1.50	0.30	8.00	22.00
7	0.80	0.15	12.50	7.20
8	0.32	0.30	8.00	15.72
9	1.50	0.05	8.00	1.25
10	2.67	0.30	8.00	16.08
11	2.20	0.45	3.50	11.08
12	0.80	0.15	3.50	3.24
13	0.80	0.45	3.50	4.77
14	1.50	0.30	0.43	3.69
15	1.50	0.30	8.00	22.99
16	1.50	0.55	8.00	2.26
17	1.50	0.30	8.00	22.74

2.4 Total Phenolic and Flavonoid Contents

The total phenolic content (TPC) was assessed through the Folin–Ciocalteu method, employing gallic acid as the reference compound, as described by Lee and Yoon (2021). Beginning with 0.1 mL of the MSPE was mixed with 0.1 mL of Folin–Ciocalteu's phenol reagent and allowed to react for 3 min. Following this, 2 mL of distilled water and 0.2 mL of 10% sodium bicarbonate were added. After being left at room temperature for 1 hour, its absorbance was measured at 725 nm using a UV–visible spectrophotometer (Shimadzu, UV-1280, Japan). A standard curve for gallic acid was created by preparing dilutions of gallic acid (0.1, 0.5, 1.0, 2.5, and 5 mg/mL), and the results were expressed in terms of milligrams of gallic acid equivalent (GAE) per gram of the extract using Equation (2). The experiment was conducted in triplicate, with distilled water serving as the control.

The analysis of the TFC was carried out following the procedure described by Lee and Yoon (2021). This involved mixing approximately 0.5 mL of the MSPE with 0.1 mL of 10% aluminum nitrate and 0.1 mL of 1 M potassium acetate. Afterward, this mixture was blended with 4.3 mL of 80% (v/v) ethanol and allowed to incubate in darkness for 40 min. Following incubation, the sample's absorbance was measured at 415 nm using a UV–visible spectrophotometer (Shimadzu, UV-1280, Japan), with naringin employed as the reference standard. The results were expressed in terms of milligrams of naringin equivalents (NE) per gram of the extract, and the analysis was performed in triplicate.

2.5 Isolation of *Trichoderma* spp. from an Infected Mushroom Bag

An infected mushroom bag was collected from the mushroom house at Block A3, UniCITI Alam Campus, UniMAP, Perlis. Using a sterile inoculum loop under laminar flow, the infected mushroom bag was isolated on a potato dextrose agar (PDA) plate. The plate was sealed, labeled, and incubated in an incubator at 30 ± 2°C for 5 days. After 5 days, the forming of green spores from the PDA plate was picked up by a sterile loop and dotted at the center of the new plates. The plate was sealed and labeled prior to the 30 ± 2°C incubation. The steps were repeated to get a pure single colony of *Trichoderma* spp.

2.5.1 Morphological Analysis of *Trichoderma* spp

Possible *Trichoderma* spp. isolates were identified through a morphological analysis. This analysis encompassed the assessment of both macromorphological and micromorphological characteristics. The macromorphological features considered included the growth rate, colony attributes (such as color, reverse color, and edge characteristics), as well as the structure and color of the mycelium. Moreover, micromorphological characteristics, like conidiation, conidia branching, shape, size, and color, in addition to phialide shape, size, and arrangement, were meticulously documented. The diameter of the *Trichoderma* spp. colonies were measured daily, and the average growth rate was analyzed. Fresh mycelium was observed under a light microscope at both 40× and 100× magnification, as per the methodology outlined by Elsherbiny et al. (2021).

2.5.2 Deoxyribonucleic Acid (DNA) Sequencing Analysis

To verify the identity of the isolates, DNA extraction, PCR amplification, and sequencing procedures were carried out for *Trichoderma* spp. Four-day-old *Trichoderma* spp. cultures grown on PDA were carefully cut out at 0.5 cm by 0.5 cm using a sterile scalpel. These excised samples were then put in a 1.5 mL microcentrifuge tube. To ensure the safety and integrity of the sample during transportation, the tube was securely wrapped with parafilm and placed within a durable protective container. Subsequently, the prepared sample was sent to Apical Scientific Sdn. Bhd. for analysis.

For DNA extraction, the cetyltrimethylammonium bromide (CTAB) method was used to extract fungal DNA (El Sobky et al., 2019). The DNA template from the sample was used in polymeric chain reaction (PCR) amplification using the agarose gel electrophoresis method, which separates DNA products based on size and charge. For PCR amplification, primer pair of internal transcribed spacer (ITS) namely ITS1 (5'TCCGTAGGTGAACCTGCCG3'), and ITS4 (5'TCCTCCGCTTATTGATATGC3') were used. The mixture contained 50 ng of the template DNA, 1.25 U Taq DNA polymerase, 1x Taq polymerase buffer, 0.5 mM of each primer, and 200 µM of each of the four deoxyribonucleotide triphosphates. The electrophoresis procedure was conducted to visualize the product before sending it to the GenBank database via the website (http://www.ncbi.nlm.nih.gov/BLAST) for product sequencing (El Sobky et al., 2019). Ultimately, the corresponding species for each isolate were identified. The identified strains were then assigned laboratory nomenclature by the established system.

After the sequences were identified, phylogenetic trees were analyzed using Molecular Evolutionary Genetics Analysis-Version 5 (MEGA5) (El Sobky et al., 2019). The analysis was performed by the Heuristic, and a tree was constructed by combining the results of 1,000 random additions and sequential additions. The reliability of the tree was calculated by a series of 1,000 replicated tests. *Trichoderma* spp. sections were analyzed using a broad phylogenetic approach to define the out-group taxa for the individual analysis.

2.6 *In vitro* analysis of MSPE against *Trichoderma* spp.

2.6.1 Antifungal activity of MSPE

For the antifungal activity, the poisoned media method was applied (Silva et al., 2021). Approximately 20 µL of *Trichoderma* spp. was dropped at the center of the PDA plate and flattened on the plate using a large glass tube. The culture was incubated for 4 days in an incubator at 30 ± 2°C.

Then, 2.5 mL of the MSPE at concentrations of 1.5, 3.0, 4.5, 6.0, 7.5, 9.0, 10.5, 12.0, 13.5, 15.0, 16.5, 18.0, 19.5, 21.0, and 22.5 mg/mL was poured into 15 mL of warm sterilized PDA plate, respectively. The plate was allowed to cool. Then, a 5 mm-diameter cylindrical fragment of *Trichoderma* spp. was placed at the center of each plate using a cork borer.

Three replicates per treatment were prepared along with the control. The plate was kept in a controlled environment in darkness for 8 days at a temperature of 30 ± 2°C. The equatorial diameter of the mycelial growth of each fungus was measured using a digital vernier caliper every 24 hours for a total of approximately 8 days. Mycelial growth inhibition was determined using Equation (3), where MGI denotes mycelial growth inhibition and MG denotes mycelial growth. NaCl served as a positive control and itraconazole, a commercial fungicide, was used as a negative control in this study. The minimum inhibition concentration (MIC) was defined as the lowest concentration of the antifungal agent needed to halt the growth of the fungus. The lethal concentration (LC) for LC_{50} and LC_{90} were concentrations at which 50% and 90% of the samples tested died, respectively, and were analyzed using the Probit Analysis method.

2.6.2 Spore germination inhibition (SGI%)

The analysis involved transferring 100 µL of a conidial suspension of *Trichoderma* spp. at a concentration of 1×10^6 CFU/mL into test tubes filled with potato dextrose broth (PDB) containing the MSPE at the MIC level. As a control, test tubes with PDB but without the MSPE were used. These tubes were then placed on a rotary shaker set at 150 rpm and maintained at a temperature of 30 ± 2°C. After 15 hours of incubation, approximately 200 spores in each treatment were microscopically examined under a light microscope. This examination was conducted to assess the germination rate and measure the length of the germ tube using a hemocytometer. The experiment was replicated twice, and each treatment was performed in triplicate. Spore germination (SG) was considered successful when the length of the germ tube equaled or exceeded the length of the spore, following the approach described by Elsherbiny et al. (2021). The percentage of spore germination inhibition was determined using Equation (4).

2.6.3. Macroscopic and microscopic analysis of isolated *Trichoderma* spp.

Three-day-old *Trichoderma* spp. on the plate were cut using a sterile blade. The color, shape, margins, elevations, texture, and other characteristics of the treated *Trichoderma* spp. with MSPE were observed and analyzed. The sterile blade was used to cut the edge of the colony into a thin layer and place it on the glass slide. Methylene blue was dropped on the sample, and the image of the samples was observed under 40× and 100× magnification under a light microscope.

2.7. Statistical analysis

The optimization of protein extraction from *M. charantia* seeds and the subsequent statistical analysis was carried out through response surface methodology (RSM) through central composite design (CCD) by using Design-Expert software (Version-12). The models and parameters were considered statistically significant when the p-value was less than 0.05. Regression analysis of the response was performed using a quadratic equation to determine the best-fitting model.

$$Total\ phenolic\ content = \frac{concentration\ of\ MSPE\ x\ volume\ of\ MSPE\ solution}{weight\ of\ extraction} \quad (2)$$

$$MGI\ (\%) = \frac{MG_{control} - MG_{treatment}}{MG_{control}}\ x\ 100 \quad (3)$$

$$SGI\ (\%) = \frac{SG_{control} - SG_{treatment}}{SG_{control}}\ x\ 100 \quad (4)$$

3. RESULTS AND DISCUSSION

3.1 Protein Optimization of MSPE using CCD

The protein concentration of *M.* charantia seeds was significantly influenced by several factors, namely NaCl concentration, solute-to-solvent ratio, and extraction time, as presented in Table 2. From the result, the protein concentration of *M. charantia* seeds varied between 1.65 and 22.99 mg/mL with a standard deviation from 0.0040 to 0.0953. It was shown that the optimum protein

concentration was obtained using a moderate concentration of NaCl and the highest values of extraction time and solute-to-solvent ratio. However, if the NaCl, time and solute-to-solvent ratio of extracted protein were extended beyond this range, it might affect the solubility and structure of the extracted protein, leading to low protein content. The optimum protein concentration of 22.99 mg/mL was obtained in run 15 (1.5 M of NaCl solution, 0.30 g/mL ratio, and sonication for 8 min). Three replicates of center points (runs 6, 15, and 17) were used to measure the pure error sum of squares. Run 4 showed the lowest protein concentration of only 1.65 mg/mL, which might be due to the long extraction time (12.5 min) that contributed to protein denaturation. Prolonging the extraction time led to the reduction of the solvent permeability due to impurities scattering around the solvent (Gadalkar and Rathod, 2020).

In addition, a low solute-to-solvent ratio (0.55 g/mL) can affect protein extraction, which causes insufficient sources for protein extraction and excess solvent, as shown in run 16, where there was only a small amount of protein obtained (2.26 mg/mL). Optimization of protein extraction increased the protein concentration of *M. charantia* seeds from 0.0593 mg/mL (Chakraborty et al., 2020) to 22.99 mg/mL (obtained in this study). Through this study, the optimized condition for the MSPE allows more protein to be extracted and produces significant improvement in protein extraction.

The fitted model proved a valuable understanding of the extraction process conditions, approximating the actual system, and confirming that all assumptions of least square regression were obeyed. To assess the fitness of variances among parameters in the optimization test, an analysis of variance (ANOVA) was employed. As detailed in Table 3, the quadratic models for both main and interaction factors exhibited significance, indicated by a p-value of <0.05, showing a highly substantial and statistically meaningful fit for each variable. Furthermore, a Fisher's test (F-value) was conducted on the experimental data to evaluate the model's statistical significance. The F-value of 450.10 indicates the model is significant, with only a 0.01% chance that a large F-value could occur because of noise. Consequently, all parameters are deemed significant, with p-values less than 0.0500 affirming the significance of model terms. Regarding the lack-of-fit analysis, the F-value of 0.84 implies that the lack of fit is not significant when compared to the inherent error. There is a 62.10% probability that a lack-of-fit F-value of this magnitude could occur due to random fluctuations.

The correlation coefficient R^2 was 0.9983, showing that the model was valid and could be accepted. In addition, only 99.83% of the total variation could be attributed to the investigated experimental variables. The "adjusted R^2" value of 0.9961 indicated a high degree of correlation between the experimental and predicted values. The "predicted R^2" of 0.9898 and the "adjusted R^2" of 0.9961 were in reasonable agreement. The low value of the coefficient of variation (5.38%) demonstrated that the experimental values were extremely precise and reliable. The "adequate precision" ratio, which measures the signal-to-noise ratio, is greater than 4 (57.38), showing that this model can be used to navigate the design space with an adequate signal.

3.2 Effect of the Main Factor for MSPE Optimization

Various extraction techniques have been reported namely maceration, digestion, Soxhlet extraction, superficial extraction, microwave-assisted extraction, and ultrasound-assisted extraction, whereby every technique has its advantages in separating the desired product from raw material. The ultrasound-assisted extraction is a powerful extraction technique that helps to enhance the yield within a short reaction time with high selectivity and minimal side effects. It breaks down the cell walls of the raw materials under substantial pressure, thereby facilitating the efficient dissolution of active plant cell ingredients in the solvent. All main factors involved in the extraction namely NaCl concentration, solute-to-solvent ratio and extraction time were significant in the protein concentration with a p-value < 0.0001 (Fig. 1).

Fig. 1(a) shows that the salt concentration (up to 1.5 M) was proportional to the protein of *M. charantia* seed extract before the protein concentration dropped down to 2.2 M. The appropriate reason is protein solubility. The solubility of proteins is influenced by salt concentration in the surrounding medium. Protein solubility can be increased by using a low salt content, whereas high salt concentrations can cause proteins to aggregate and precipitate out of the medium. In addition, high salt concentrations can disrupt or enhance protein-protein interactions. Proteins that typically interact with one another may dissociate, affecting the ratios of these proteins in the extracted sample. Besides, some proteins are specifically dependent on salt for their stability or function. High salt concentrations can lead to denaturation or other structural changes, affecting the types of proteins extracted (Mao et al., 2007; Hu et al., 2017, Zhang et al., 2019).

Fig. 1(b) further demonstrates that the solute-to-solvent ratio is proportional to the protein concentration up to 3.0 g/mL. Unfortunately, the pattern turns down after reaching 3.0 g/mL. The valid reason is that a higher solute-to-solvent ratio typically leads to a higher concentration of the extracted compounds in the solvent. However, it also causes saturation, where the solvent can no longer dissolve more solute. Beyond this point, adding more solute will not increase extraction yields. This is especially relevant for solvents that have limited solubility for a particular solute (Gadalkar and Rathod, 2020).

Fig. 1(c) shows that the MSPE was increased when the extraction time increased from 3.5 to 8.0 min before it dropped down due to the protein denaturation. It expresses the importance of optimizing the extraction time as this

factor affects both the overall cost of the operation and the efficiency of the extraction (Ozturk et al., 2018). A short extraction period leads to insufficient time for the ultrasound to break the cell, consequently making less cell permeability in the solvent (Drevelegka and Goula, 2020). Apart from that, a long extraction period may lead to protein denaturation. Therefore, the best extraction time helps in optimizing the extraction of bioactive compounds. The pattern obtained obeys Fick's law, which states that ultimate equilibrium is obtained between the matrix solid and the extractant after a given contact period and that no further extraction efficiency is gained for extended durations (Ozturk et al., 2018). The previous study proved that the long extraction period reduced the anthocyanin compound (Gadalkar and Rathod, 2020).

According to the main factor analysis, the MSPE increased when the NaCl concentration, solute-to-solvent ratio, and extraction time were increased from 0.8 to 1.5 M, 0.15 to 0.3 g/mL, and 3.5 to 8.0 min before the MSPE began to drop. Aside from the effect of the main factor, the interaction of the parameters on MSPE content was also investigated.

Table 3. ANOVA analysis of MSPE

Source	Sum of squares	Degree of freedom	Mean	F-value	p-value	Remarks
Model	967.83	9	107.54	450.10	<0.0001	significant
A - NaCl concentration	2.29	1	2.29	9.58	0.0174	
B - ratio (solute-to-solvent)	2.06	1	2.06	8.64	0.0217	
C - extraction time	7.27	1	7.27	30.43	0.0009	
AB	2.27	1	2.27	9.51	0.0177	
AC	30.30	1	30.30	126.84	<0.0001	
BC	6.46	1	6.46	27.06	0.0013	
A^2	63.43	1	63.43	265.48	<0.0001	
B^2	613.09	1	613.09	2566.15	<0.0001	
C^2	560.31	1	560.31	2345.24	<0.0001	
Residual	1.67	7	0.2389			
Lack of fit	1.13	5	0.2269	0.8437	0.621	not significant
Pure error	0.5379	2	0.2689			
Cor total	969.5	16				
R^2	0.9983					
Adj R^2	0.9961					
Pred R^2	0.9896					
Coefficient of variance (%)	5.38					
Adeq. precision	57.38					

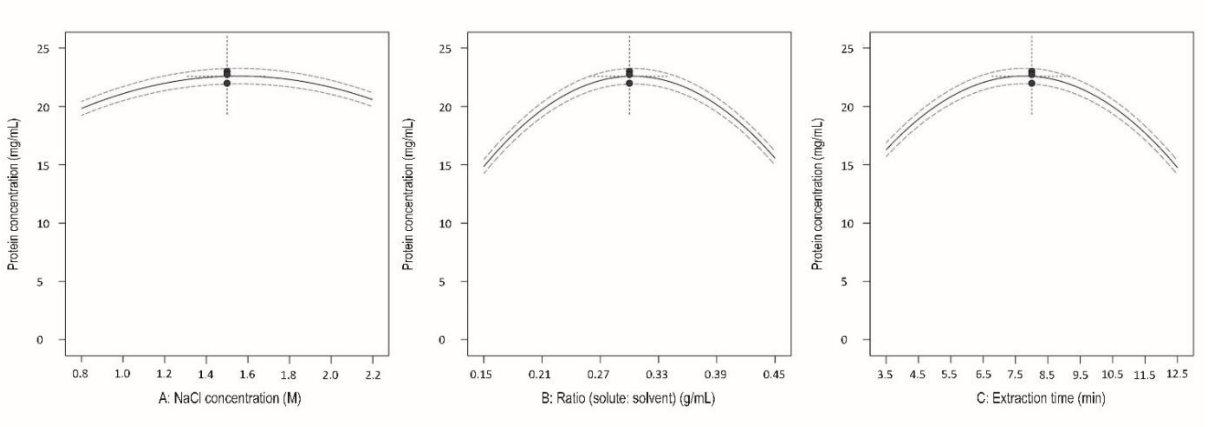

(a) (b) (c)

Fig. 1. Main factor plots for (a) NaCl concentration, (b) solute-to-solvent ratio, and (c) extraction time

3.3 Effect of Interaction for MSPE Optimization

Using the polynomial equation derived from the regression analysis, the relationship between the independent variables (NaCl concentration, solute-to-solvent ratio, and extraction time) and the dependent variable (protein concentration) was visually represented in a three-dimensional response plot. The response surface contour plot illustrates the interaction between two variables while keeping the third variable at its optimal setting.

Fig. 2(a) shows the interaction between NaCl concentration and solute-to-solvent ratio at constant extraction time. The protein concentration was low when NaCl concentration and solute-to-solvent ratio were low, however gradually increased when the NaCl increased from 1 to 1.5 M and solute-to-solvent ratio increased from 0.15 g/mL to 0.3 g/mL and reached the maximum of protein at 1.5 M NaCl and 0.3 g/mL solute-to-solvent ratio. The protein concentration is low beyond this range, which might be due to the high NaCl resulting in protein denaturation.

At a constant solute-to-solvent ratio, (Fig. 2(b)) too low or too high extraction time and NaCl concentration resulted in a decrease in protein concentration. The value progressively increased as the extraction time and NaCl concentration increased from 3.5 to 8.0 min and 0.8 to 1.5 M, respectively, peaking at 8.0 min and 1.5 M. Nonetheless, the protein concentration started to decrease beyond this range. This might be due to the prolonging of the extraction time promoted protein degradation.

At a constant NaCl concentration, the interaction between extraction time and solute-to-solvent ratio displays similar observations. The MSPE increased as the extraction time and solute-to-solvent ratio were increased from 3.5 to 8.0 min and 0.15 to 0.45 g/mL, respectively, and reached maximum protein concentration at 8.0 min and 0.3 g/mL. The protein was decreased beyond that range due to the high solute-to-solvent ratio impeding the dispersion of the solvent in the sample, thereby reducing the efficiency of the extraction process. Conversely, a low solute-to-solvent ratio results in inefficiency on an industrial scale due to the substantial solvent consumption and limited sample processing per unit of time (Drevelegka and Goula, 2020; Gullon et al., 2020).

3.3.1 Numerical optimization

The numerical optimization aims to optimize the process of MSPE. The input variables (NaCl concentration, solute-to-solvent ratio and time of extraction) were set at optimum levels with 95% confidence levels. The optimum of MSPE with 98.4% desirability was predicted at a NaCl concentration of 1.58 M, a solute-to-solvent ratio of 0.30 mg/mL, and an extraction time of 7.68 min, with a predicted MSPE value of 22.64 mg/mL (Table 4). The setting of the optimum MSPE model was validated in five replications of the experimental run. The experimental MSPE value was 22.80 mg/mL, with a standard deviation of 0.118 (standard deviation < 2), indicating that the experimental and predicted values corresponded well. Therefore, the optimized condition for MSPE was at 1.58M NaCl, 0.30 g/mL solute-to-solvent ratio and 7.68 min of extraction time.

3.4 Total Phenolic and Flavonoid Contents of MSPE

Phenolic compounds are a broad group of phytochemicals that include one or multiple phenol groups. Phenols play a crucial role in determining the color, flavor, and taste of numerous herbs commonly utilized in drinks and food. These secondary metabolites are highly known for their pharmacological activities. Since phenols have several beneficial pharmacological effects, including antioxidant, antibacterial, anti-inflammatory, and anticancer qualities, they are frequently used in a broad variety of pharmaceuticals (Kaushik et al., 2021).

From the highest protein of MSPE in Table 1, the samples were evaluated for the yield of TPC and TFC. The phenolic content was assayed based on Folin-Ciocalteu reagent and the content of TPC in MSPE extract was 16.45 mg GAE/g extract. Nonetheless, the flavonoid content was determined based on aluminum nitrate colorimetric assay and the content of TFC in MSPE extract was 5.78 mg NE/g extract. These findings align with a prior investigation, which reported that the TPC and TFC values of *M. charantia* are 18.73 mg GAE/g extract and 8.29 mg NE/g extract, respectively (Lee and Yoon, 2021). The notable levels of TPC and TFC serve as a strong indicator of the MSPE's efficacy as an antifungal agent. The TPC and TFC compounds work together with the antifungal protein in the alpha-momorcharin compound and boost the antifungal properties of MSPE consequently inhibiting the growth of *Trichoderma* spp.

The application of UAE especially ultrasonic probes allows extracts with greater TPC and TFC values when compared to ultrasonic water bath and other methods. This occurrence can be ascribed to the generation of bubbles via cavitation caused by ultrasonic waves, which disrupt the cell wall, leading to greater elution and solubility of chemicals within the cell (Lee and Yoon, 2021). Another reasonable reason, the ultrasonic water bath is placed at the bottom of the ultrasonic bath and transmits energy to the sample indirectly through the medium whereas, in the ultrasonic probe, energy is transferred directly to the sample by ultrasonic waves generated from the probe, leading to heightened ultrasonic performance. This direct delivery of energy may be a key factor contributing to the higher TPC and TFC values achieved through the ultrasonic probe method, as elucidated by Lee and Yoon (2021).

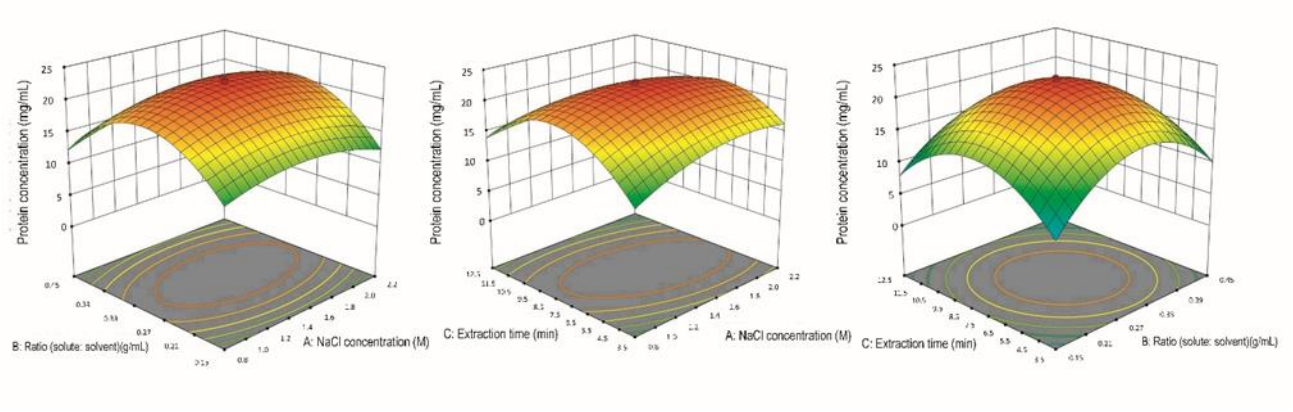

(a) (b) (c)

Fig. 2. Interaction between (a) NaCl concentration-ratio (b) NaCl concentration-extraction time and (c) ratio-extraction time for optimized MSPE

Table 4. Optimal conditions and the predicted and experimental value of MSPE

A (M)	B (g/mL)	C (min)	Predicted MSPE (mg/mL)	Experimental MSPE (mg/mL)	σ, STD
1.58	0.30	7.68	22.64	22.80	0.118

A: concentration of NaCl, B: solute-to-solvent, C: time of extraction

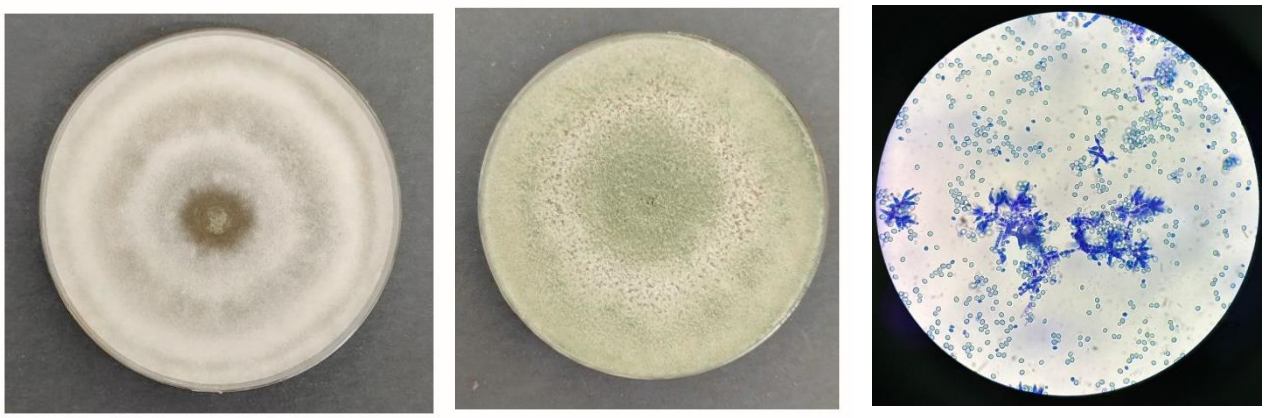

(a) (b) (c)

Fig. 3. Macroscopic observation of *Trichoderma* spp. (a): 3 days old (b) 6 days old (c) microscopic observation of *Trichoderma* spp.

Table 5. The colony and mycelial characteristics of *Trichoderma* spp.

Strain	Colony					Mycelial	
	Texture	Color	Reverse color	Edge	Diameter (mm)	structure	Color
TH001	Floccose	White to green	Creamish	Wavy	80	Concentric zones	White

3.5 Identification of *Trichoderma* spp.

3.5.1 Macroscopic and microscopic observations on *Trichoderma* spp

The isolates of *Trichoderma* spp. TH001 was characterized. The isolates' macroscopic features such as colony morphology (texture, color, reverse color, edge, and diameter) and mycelial (structure and color), are shown in Fig. 3 and Table 5. Fig. 3 shows the difference in growth of *Trichoderma* spp. during the lag and log phase as well as the morphological characteristic of *Trichoderma* spp. TH001 under the light microscope. At the initial phase, the white mycelium of the isolates was rapidly growing, as shown in Fig. 3(a), which later became green as the result of sporulation and showed the formation of a concentric ring that is typical of *Trichoderma* spp. colonies, as shown in Fig. 3(b). The green conidia were interspersed within the white mycelium. The color attribute aligns with the characteristics mentioned previously (El Sobky et al., 2019; Kumar et al., 2020). In addition, the colonies exhibited a

floccose shape with an average diameter of 80 mm, displayed a wavy pattern, and had a cream color on the underside.

Microscopic features such as conidia (conidiation, branching, shape, size, and color) and phialide characteristics (shape, size, and disposition) were characterized, as shown in Table 5. The microscopic features of *Trichoderma* spp. showed that the mycelium consists of hyphae that are hyaline, highly branched, and septate (Fig. 3(c)). The isolates developed hyaline mycelia, and the presence of conidiophores was noted on the third day of incubation. The conidia were 3.0–7.0 mm in diameter, mostly ellipsoidal in shape, and either green or hyaline in color. Phialides were 3.0–7.00 µm in size and were lageniform and bowling pin in shape. Moreover, the cell wall was intact along the hyphae and the conidiophore was rough and spiny. The microscopic observation outcomes are aligned with prior studies (El Sobky et al., 2019; Kumar et al., 2020).

3.5.2 Neighbor-joining phylogenetic tree

There were many types of colonies in infected mushroom bags and the distinctive sporulation pattern mostly toward the type of dominating fungus that grow on the mushroom bags. Hence, the dominating fungus on the infected site was plated on PDA media for molecular identification. Although colony morphology served as the ability to differentiate between species of this fungus was insufficient for its identification, necessitating the use of molecular methods to confirm the precise species (El Sobky et al., 2019; Kumar et al., 2020). Molecular techniques are among the most accurate means of distinguishing techniques between species and identifying novel strains. In particular, DNA sequence comparison allows precise species identification and reveals insights into the evolutionary and ecological connections between different species (El Sobky et al., 2019; Kumar et al., 2020).

Therefore, ITS sequences were used for species-level identification of *Trichoderma* spp. TEF1-sequencing analysis could also verify species classification. As shown in Fig. 4, there were four main *Trichoderma* species present, having high similarity identification from the laboratory nomenclature system. All the fungi have above 99% cluster similarities with the sequence from GenBank. They were *Trichoderma* sp. ZH1 (Accession no.: DQ282127.1, genetic similarity:99.51%), *Hypocrea lixii* (Accession no.: DQ445808.1, genetic similarity: 99.68%), *Trichoderma amazonicum* (Accession no.: MH864268.1, genetic similarity: 99.67%) and *Trichoderma pleuroticula* (Accession no.: EU280071.1, genetic similarity: 99.19%). From the analysis, the closest one was *Trichoderma* sp. ZH1. Even though *Hypocrea lixii* has high sequence similarity, however, it was a teleomorph of a complex multispecies of *Trichoderma harzianum* that has more than thirteen species (Katoch et al., 2019).

3.6. *In vitro* Study of MSPE Against *Trichoderma* sp. ZH1

3.6.1 Effect of the MSPE on mycelial growth inhibition (MGI)

The antifungal activity of the MSPE is evaluated on *Trichoderma* sp. ZH1 in terms of mycelium growth zone diameter (mm), mycelium inhibition rate (%), and sporulation inhibition as shown in Table 6. The positive control (Itraconazole) strongly inhibits sporulation and *Trichoderma* sp. ZH 1 mycelium growth by 94.83%. In comparison to the negative control, the fungus grows normally and covers the plate with green spores. The MGI *Trichoderma* sp. ZH1 was increased proportionally with the MPSE concentration. The inhibition rate was started at a concentration of 7.50 mg/mL of MSPE and remained consistent up to 10.5 mg/mL with visible spore production. Nevertheless, when the concentration of MPSE was 12.0 mg/mL or higher, there was no sporulation and the MGI became more significant with 52.91% inhibition and was further increased to 75.44% after treatment with 22.50 mg/mL. The minimum inhibition concentration (MIC) of MSPE was determined to be 7.50 mg/mL, a point which was the minimum concentration of MSPE started to inhibit the growth of *Trichoderma* sp. ZH1. From the concentrations range from 1.5 mg/mL to 22.50 mg/mL as displayed in Table 6, the data were extrapolated and analyzed using Probit Analysis, for the LC_{50} and LC_{90} analysis. It was found that the concentration required to inhibit 50% and 90% of *Trichoderma* sp. ZH1 were 13.62 and 24.97 mg/mL, respectively.

A macroscopic view of mycelium growth for *Trichoderma* sp. ZH1. on potato dextrose agar (PDA) was carried out following four days of incubation, as shown in Fig. 5. The mycelium of the negative control (0 mg/mL) grew rapidly from white to green with a ring zone until it completely covered the plate on day three before further continuing with the sporulation process (Fig. 5(a)). Nevertheless, even though they had tiny mycelium growth, however, there was no sporulation of *Trichoderma* sp. ZH1 after being treated with 13.62 and 22.50 mg/mL of the MSPE respectively (Figs. 5(b) and 5(c)). It demonstrates that the MSPE effectively inhibited the growth of *Trichoderma* sp. ZH1. The MSPE might break down the septum in the cell wall of hyphae and inhibit the sporulation, consequently affecting the growth of *Trichoderma* spp. (Villarreall-La et al., 2020; Oyelere et al., 2022).

3.6.2. Effect of the MSPE on spore germination inhibition (SGI)

Spore germination inhibition (SGI) was conducted to support the MGI analysis and was performed between the control (negative and positive) and treated samples (13.62 mg/mL and 22.50 mg/mL). After 15 hours incubating the *Trichoderma* sp. ZH1 with different MSPE concentrations,

the first signs of spore germination were observed. The MSPE affects spore germination rate in a concentration-dependent manner where the SGI increases as the MSPE increases (Fig. 6). The SGI for the negative and positive control were 0% and 95% respectively indicating the *Trichoderma* sp. ZH1 was germinated well under a normal condition and achieved almost full inhibition after treatment with itraconazole. After treatment with MSPE at 13.62 mg/mL and 22.50 mg/mL, the SGI was statistically significant ($p < 0.001$) with 55% and 69% inhibition respectively. The MSPE at 13.62 mg/mL was shown to successfully inhibit half of the spore germination of *Trichoderma* sp. ZH1.

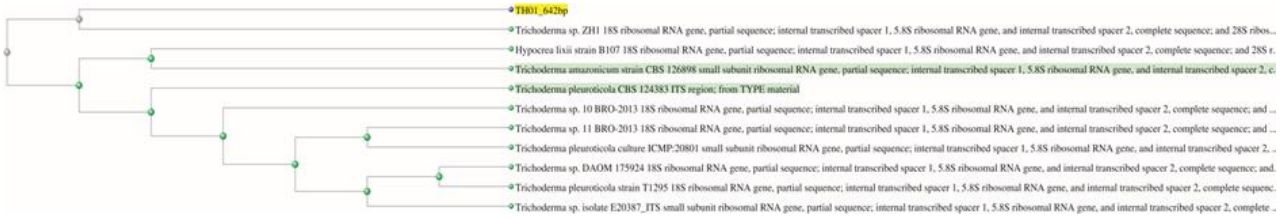

Fig. 4. Neighbor-joining phylogenetic tree of *Trichoderma* strains created using the MEGA5 program, utilizing internal transcribed spacer rDNA (ITS) sequences.

Table 6. *Trichoderma* sp. ZH1 mycelial growth and sporulation inhibition

Sample	MSPE (mg/mL)	Growth zone diameter (mm)	Inhibition rate (%)	Spore production
1	Negative control	85	0	Yes
2	Positive control	4.393	94.83	No
3	1.50	85.00	0	Yes
4	3.00	85.00	0	Yes
5	4.50	85.00	0	Yes
6	6.00	85.00	0	Yes
7	7.50	80.29	5.55	Yes
8	9.00	51.80	39.06	Yes
9	10.50	47.71	43.87	Yes
10	12.00	44.07	48.16	No
11	13.50	40.03	52.91	No
12	15.00	25.03	58.79	No
13	16.50	28.70	66.24	No
14	18.00	27.18	68.09	No
15	19.50	25.03	70.07	No
16	21.00	23.70	72.08	No
17	22.50	20.65	75.44	No

*Percentage of growth inhibition was calculated by:
(Colony diameter of −ve control − colony diameter at stationary phase)/Diameter of −ve control) × 100.
*Itraconazole 100 mg was used in +ve control plate.

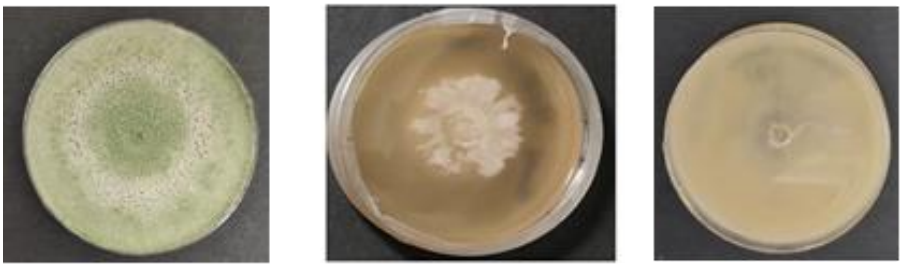

(a) (b) (c)

Fig. 5. Macroscopic view of mycelium growth of *Trichoderma* sp. ZH1 after four days of incubation in (a) MSPE : 0 mg/mL (b) MSPE: 13.62 mg/mL, and (c) MSPE: 22.50 mg/mL

The sporulation process plays a main role in the life cycle of fungi for their reproduction and survival in challenging environmental conditions (Huang and Hull, 2017). The MPSE demonstrated the ability to inhibit the sporulation and growth of *Trichoderma* sp. ZH1. This is consistent with prior studies, where protein concentration

has been proven to trigger apoptosis in fungi, which contributes to the antifungal properties (Zhu et al., 2013; Citores et al., 2022; Citores and Ferreras, 2023). In addition, plant extracts can inhibit spore production, fungal growth, cell wall-degrading enzymes, stress response proteins, antioxidant and detoxification enzymes, and metabolic processes such as thiamine biosynthesis, which consequently inhibit fungal growth (Al-Ani et al., 2018; Citores and Ferreras, 2023).

Previous research confirmed that bioactive compounds such as polyphenolic extract from *Parastrephia lepidophylla* influenced the spore germination of *P. digitatum* and *Geotrichum citri-aurantii* (Ruiz et al., 2016). From this finding, preventing germination would prevent fungal growth and subsequent spoilage. Therefore, it is highly desirable to inhibit the viable conidia by administering conidia-inactivating products such as MSPE.

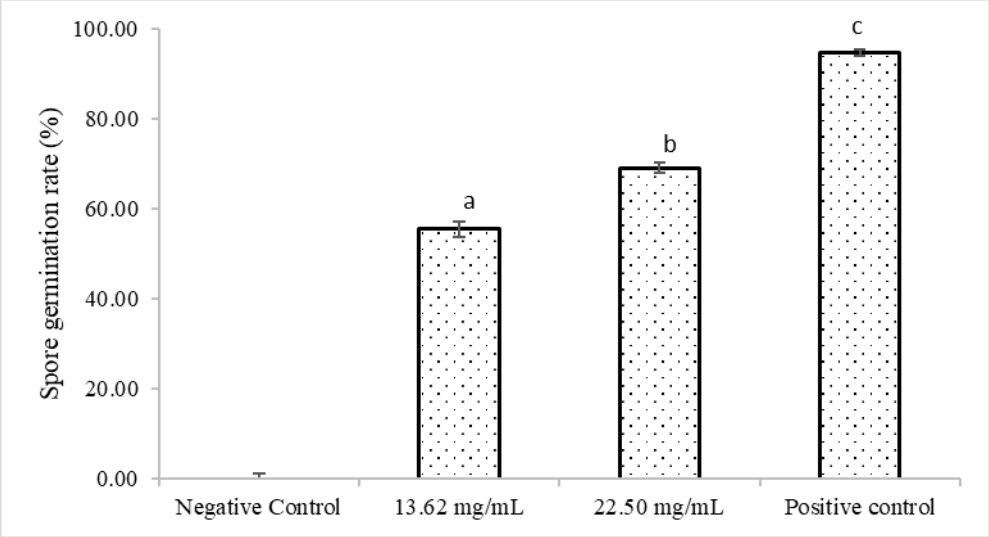

Fig. 6. Effect of spore germination inhibition (SGI) on *Trichoderma* sp. ZH1.

4. CONCLUSION

The optimized *M. charantia* seed protein extract (MSPE) was obtained through ultrasonic-assisted extraction (UAE) with 1.58 M NaCl, using a solute-to-solvent ratio of 0.3 g/mL, and 7.68 min of extraction time. The yield of the optimized MSPE was measured at 22.80 mg/mL. All three parameters, including NaCl concentration, solute-to-solvent ratio, and extraction time, were discovered to have a crucial role in MSPE extraction. The isolated fungal from the infected mushroom bag was identified as *Trichoderma* sp. ZH1 (Accession no.: DQ282127). In antifungal analysis, it was observed that the MSPE exhibited strong antifungal activity and provided effective protection against *Trichoderma* sp. ZH1 infection. The maximum inhibition rate was 75.44% at 22.50 mg/mL of MSPE. This suggests that the MSPE could be a viable alternative to chemical fungicides for controlling *Trichoderma* sp. ZH1 infections in mushroom cultivation. Moreover, the antifungal properties of the MSPE may extend to combat green mold diseases on other crops. The research finding innovation highlights the converting waste from *M. charantia* seeds into a potent antifungal agent. It provides a green alternative to antifungal to cater to the infection of green mold disease in mushroom cultivation, which in return can enhance the quantity and quality of mushrooms. Further development of the biofungicide including pilot test analysis is necessary as this eco-friendly biofungicide supports the sustainable eco-agrosystem and is in line with the Sustainable Development Goal (SDG) for Zero Hunger.

ACKNOWLEDGMENT

This research work was supported by the Fundamental Research Scheme (FRGS) under grant number FRGS/1/2019/STG 05/UNIMAP/02/03 from the Ministry of Higher Education Malaysia. The authors would like to appreciate the help and support from the Faculty of Chemical Engineering & Technology, University Malaysia Perlis, Malaysia.

REFERENCES

Al-Ani, B.M., Owaid, M.N., Al-Saeedi, S.S.S. 2018. Fungal interaction between *Trichoderma* spp. and *Pleurotus ostreatus* on the enriched solid media with *Licorice glycyrrhiza glabra* root extract. Acta Ecologica Sinica, 38, 268–273.

Azmir, J., Zaidul, I.S.M., Rahman, M.M., Sharif, K.M., Mohamed, A., Sahena, F., Jahurul, M.H.A., Ghafoor, K., Norulaini, N.N.N., Omar, A.K.M. 2019. Techniques for extraction of bioactive compounds from plant materials: A review. Journal of Food Engineering, 117, 426–436.

Bellettini, M.B., Fiorda, F.A., Maives, H.A., Teixeira, G.L., Avila, S., Hornung, P.S., Junior, A.M., Ribani, R.H. 2019. Factors affecting mushroom Pleurotus spp. Saudi Journal of Biological Sciences, 26, 633–646.

Bhatta, U.K. 2021. Alternative management approaches of citrus diseases caused by *Penicillium digitatum* (green mold) and *Penicillium italicum* (blue mold). Frontier of Plant Science, 12, 833328.

Chakraborty, S., Uppaluri, R., Das, C. 2020. Optimization of ultrasound-assisted extraction (UAE) process for the recovery of bioactive compounds from bitter gourd using response surface methodology (RSM). Food and Bioproduct Process, 120, 114–122.

Chemat, F., Rombaut, N., Sicaire, A-G., Meullemiestre, A., Fabiano-Tixier, A-S., Abert-Vian, M. 2017. Ultrasound-assisted extraction of food and natural products. Mechanisms, techniques, combinations, protocols and applications. Ultrasonics Sonochemistry, 34, 540–560.

Chen, Y.J., Zhu, J-Q., Fu, X-Q., Su, T., Li, T., Guo, H., Zhu, P-L., Lee, S. K-W., Yu, H., Tse, A. K-W., Yu, Z-L. 2019. Ribosome-inactivating protein α-momorcharin derived from the edible plant *Momordica charantia* induces inflammatory responses by activating the NF-Kappa B and JNK pathways. Toxins, 11, 694.

Citores, L., Ferreras, J.M., 2023. Biological activities of ribosome-inactivating proteins. Toxins, 15, 35.

Citores, L., Velletta, M., Singh, V.P., Pedone, P.V., Iglesias, R., Ferreras, J.M., Chambery, A., Russo, R. 2022. Deciphering molecular determinants underlying *Penicillium digitatum*'s response to biological and chemical antifungal agents by Tandem Mass Tag (TMT)-Based High-Resolution LC-MS/MS. International Journal of Molecular Science, 23, 680.

Drevelegka, I., Goula, A.M. 2020. Recovery of grape pomace phenolic compounds through optimized extraction and adsorption processes. Chemical Engineering & Processing Process Intensification, 149, 107845.

El Sobky, M.A., Fahmi, A.I., Eissa, R.A., El-Zanaty, A.M. 2019. Genetic characterization of *Trichoderma* spp. isolated from different locations of Menoufia, Egypt and assessment of their antagonistic ability. Journal of Microbiol & Biochemical Technology, 11, 409.

Elsherbiny, E.A., Dawood, D.H., Safwat, N.A. 2021. Antifungal action and induction of resistance by β-aminobutyric acid against *Penicillium digitatum* to control green mold in orange fruit. Pesticide Biochemistry and Physiology, 171, 104721.

Gadalkar, S.M., Rathod, V.K. 2020. Extraction of watermelon seed proteins with enhanced functional properties using ultrasound. Preparative Biochemistry & Biotechnology, 50, 133–140.

Gullón, P., Gullon, B., Romani, A., Rocchetti, G., Lorenzo, J.M. 2020. Smart advanced solvents for bioactive compounds recovery from agri-food by-products: A review. Trends in Food Science & Technology, 101, 182–197.

Horax, R., Hettiarachchy, N., Kannan, A., Chen, P. 2011. Protein extraction optimisation, characterisation, and functionalities of protein isolate from bitter melon (*Momordica charantia*) seed. Food Chemistry, 124, 545–550.

Hu, H., Fan, T., Zhao, X., Zhang, X., Sun, Y., Liu, H. 2017. Influence of pH and salt concentration on functional properties of walnut protein from different extraction methods. Journal of Food & Science Technology, 54, 2833.

Huang, M., Hull, C.M. 2017. Sporulation: how to survive on planet Earth (and beyond). Current Genetics, 63, 831–838.

Katoch, M., Singh, D., Kapoor, K.K., Vishwakarma, R.A. 2019. *Trichoderma lixii* (IIM-B4), an endophyte of Bacopa monnieri L. producing peptaibols. BMC Microbiology, 19, 98.

Kaushik, B., Sharma, J., Yadav, K., Kumar, P., Shourie, A. 2021. Phytochemical properties and pharmacological role of plants: secondary metabolites. Biosciences Biotechnology Research Asia, 18, 23–35.

Kumar, G., Singh, A., Pandey, S., Singh, J., Chauchan, S.S., Srivastava, M. 2020. Morphomolecular identification of *Trichoderma* sp. and their mycoparasitic activity against soil born pathogens. International Journal of Bio-resource and Stress Management, 11, 613–627.

Lee, J.J., Yoon, K.Y. 2021. Optimization of ultrasound-assisted extraction of phenolic compounds from bitter melon (*Momordica charantia*) using response surface methodology. CyTA-Journal of Food, 19, 721–728.

Mao, Y-J., Sheng, X-R., Pan, X-M. 2007. The effects of NaCl concentration and pH on the stability of hyperthermophilic protein Ssh10b. BMC Biochemistry, 8, 28.

Oyelere, S.F., Ajayi, O.H., Ayoade, T.E., Pereira, G.B.S., Owoyemi, B.C.D., Ilesanmi, A.O., Akinyemi, O.A. 2022. A detailed review of the phytochemical profiles and anti-diabetic mechanisms of *Momordica charantia*. Heliyon, 8, e09253.

Ozturk, B., Parkinson, C., Gonzalez-Miquel, M. 2018. Extraction of polyphenolic antioxidants from orange peel waste using deep eutectic solvents. Separation & Purification Technology, 206, 1–13.

Ruiz, M.D.P., Ordóñez, R.M., Isla, M.I., Sayago, J.E. 2016. Activity and mode of action of *Parastrephia lepidophylla* ethanolic extracts on phytopathogenic fungus strains of lemon fruit from Argentine Northwest. Postharvest, Biology & Technology, 114, 62–68.

Santra, H.K., Banerjee, D. 2020. Natural products as fungicide and their role in crop protection. In Singh, J., Yadav, A. (eds.) Natural Bioactive Products in Sustainable Agriculture, Springer, Singapore.

Silva, A.V., Yerena, L.R., Necha, L.L.B. 2021. Chemical profile and antifungal activity of plant extracts on *Colletotrichum* spp. isolated from fruits of *Pimenta dioica* (L.) Merr. Pesticide Biochemistry and Physiology, 179, 104949.

Tan, S.P., Stathospoulos, C., Parks, S., Roach, P. 2014. An optimised aqueous extract of phenolic compounds from bitter melon with high antioxidant capacity. Antioxidants, 3, 814.

Villarreal-La, Torre, V.E., Guarniz, W.S., Silva-Correa, C., Cruzado-Razco, L., Siche, R. 2020. Antimicrobial activity and chemical composition of *Momordica charantia*: A review. Pharmacognosy Journal, 12, 213–222.

Wang, S., Zheng, Y., Xiang, F., Li, S., Yang, G. 2016. Antifungal activity of *Momordica charantia* seed extracts toward the pathogenic fungus *Fusarium solani* L. Journal of Food and Drug Analysis, 24, 881–887.

Zhang, Y., Zhu, C., Liu, F., Yuan, Y., Wu, H., Li, A. 2019. Effects of ionic strength on removal of toxic pollutants from aqueous media with multifarious adsorbents: A review. Science of Total Environment, 646, 265–279.

Zhu, F., Zhang, P., Meng-Y, F., Xu, F, Zhang, D-W., Cheng, J., Lin, H-H., Xi, D-H. 2013. Alpha-momorcharin, a RIP produced by bitter melon, enhances defense response in tobacco plants against diverse plant viruses and shows antifungal activity in vitro. Planta, 237, 77–88.